Review

Israel Journal of Chemistry

DOI: 10.1002/ijch.201900097

A Dinucleating Ligand System with Varying Terminal Donors to Mimic Diiron Active Sites

Stephan Walleck[a] and Thorsten Glaser*[a]

Abstract: To mimic dinuclear active sites of metalloproteins, we have developed a dinucleating ligand system consisting of two tetradentate tripodal ligand compartments with varying terminal donors (carboxylates, phenolates, and pyridines). These ligands provide access to a series of μ-oxo-bridged diferric complexes. The spectroscopic study allows to investigate the molecular structures even in solution, *e.g.* depending on protonation/deprotonation of coordinated OH^- and H_2O ligands or to observe a reversible pH-dependent carboxylate-shift between terminal and bridging binding mode. The electrochemical behavior is strongly influenced by the exogenous ligands, *e.g.* OH^- facilitates oxidation to Fe^{IV} by 690 mV relative to Cl^-. Using the terminal carboxylates and a $\{Fe^{III}(\mu\text{-}O)_2Fe^{III}\}$ core even allows oxidation with O_2 to a high-valent species with Fe^{IV} ($S=2$). The implications of this study for further generation of high-valent or peroxo species and their utilization in catalysis is discussed.

Keywords: Bioinorganic Chemistry · Diiron Complexes · UV-Vis-NIR Spectroscopy · Mössbauer spectroscopy · Electrochemical Characterization

1. Introduction

Some metalloproteins use a non-heme diiron active site,[1–3] *e.g.* the oxygen transport protein hemerythrin,[4–6] ribonucleotide reductase[7,8] that catalyzes the formation of desoxyribonucleotides from ribonucleotides in DNA synthesis, or methane monooxygenase[9–15] that oxidizes methane to methanol with O_2 as external oxidant.[11,16,17] In the last two decades more metalloproteins with a diiron active site have been identified and studied.[18–22] Biomimetic model chemistry was essential to understand the structural and spectroscopic signatures and the reactivities of the metalloproteins (hypothetical and structural model complexes). Moreover, the interesting reactivities of these enzymes have attracted bioinorganic chemists to apply the knowledge gained from the natural systems for the development of new homogenous catalysts (functional model complexes). This review is not intended to summarize all the significant contributions that have been made during the last decades (for an overview, we refer to some classical[23–31] and some recent reviews[3,16,31–36]) but the focus is on a new dinucleating ligand system with varying terminal donors to mimic the active sites of non-heme diiron metalloproteins

2. The Dinucleating Ligand System

The new dinucleating[37–44] ligand system is based on the tetramine backbone **1** and the first published ligands of this system are shown in Scheme 1. The ligands differ by the terminal donors. Three different terminal donors were chosen. In order to mimic the carboxylate-rich coordination in many diiron metalloenzymes, we synthesized the ligand H_4julia.[45,46] The pyridine donors in susan/susan^{Me}[45,47,48] reflect the coordination environment in the plethora of diiron model complexes synthesized with tpa-based ligands.[49–61] On the other hand, the phenolates in H_4hilde^{Me_2}[45] have been chosen to increase the electron density by the strong σ- and π-donating phenolate ligands that should facilitate the oxidation to high-valent species.[45,62,63] Starting from the tetramine **1**, the phenolate donors in H_4hilde^{Me_2} were attached by a Mannich-reaction,[45] the carboxylate donors in H_4julia by a nucleophilic substitution,[46] and the pyridine donors in susan/susan^{Me} by a reductive amination.[45,48]

3. A Series of μ-Oxo-Bridged Diferric Complexes: Syntheses and Structures

The syntheses of μ-oxo-bridged diferric complexes with the four different ligands required varying conditions and resulted in quite some differences in the molecular structures. Reactions of the phenolate containing ligand H_4hilde^{Me_2} with a Fe^{III}

[a] *Dr. S. Walleck, Prof. Dr. T. Glaser*
Lehrstuhl für Anorganische Chemie I, Fakultät für Chemie, Universität Bielefeld, Universitätsstrasse 25, D-33615 Bielefeld, Germany
Fax: +49-521-106-6003
E-mail: thorsten.glaser@uni-bielefeld.de

Israel Journal of Chemistry

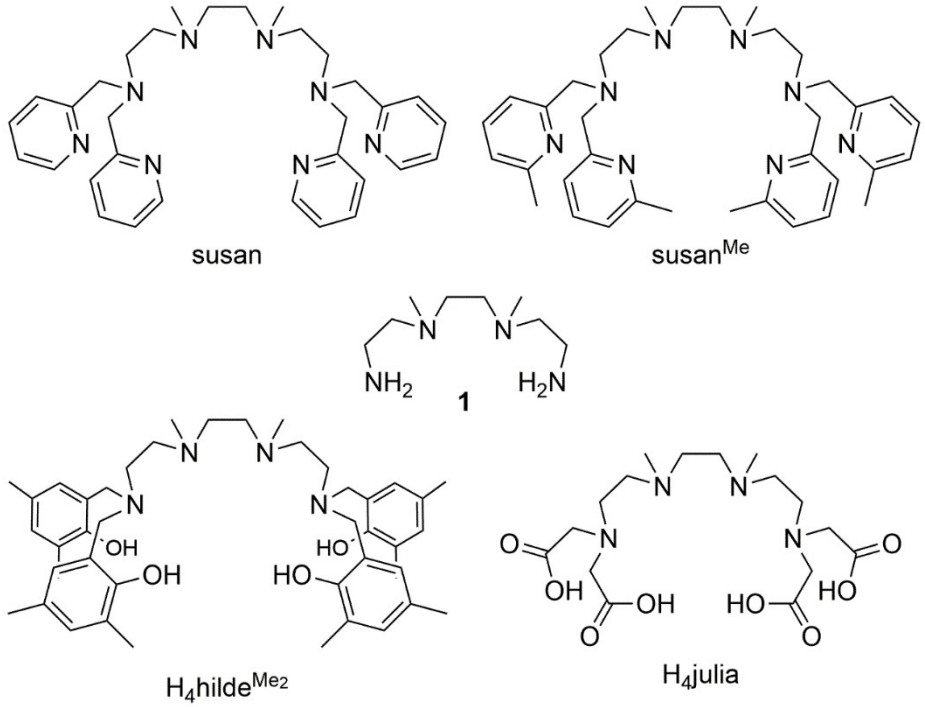

Scheme 1. The dinucleating ligand system based on the tetramine **1** with varying terminal donors.

source under basic conditions in an alcoholic solvent provide the complex [(hilde^{Me_2}){Fe(μ-O)Fe}] with the Fe^{III} ions in a five-coordinate trigonal-bipyramidal environment (Figure 1a).[45] With related mononucleating ligands,[62–65] μ-oxo-bridged diferric complexes with five-coordinate square-pyramidal coordination environment were obtained. The reaction of the ligand H_4julia with an Fe^{III} source is best performed in aqueous solution under slightly basic conditions and provides the μ-oxo-bridged complex [(julia){Fe(OH_2)(μ-O)Fe(OH_2)}] (Figure 1b).[46] The presence of alkali metal ions should be avoided as they tend to coordinate to the already coordinated carboxylate ligands resulting in oligomeric structures. The lower electron density donation of the carboxylates than of the phenolates in [(hilde^{Me_2}){Fe(μ-O)Fe}] is reflected by the need for six-coordination with exogenous terminal H_2O ligands.[45,46] For the reaction with the ligand susan, a Fe^{II} source and the presence of an anionic ligand as Cl^- is necessary. Performing the reaction in alcoholic solvent under basic atmospheric conditions provides the μ-oxo-bridged complex [(susan{FeCl(μ-O)FeCl}](ClO_4)$_2$ (Figure 1c).[45] In contrast, with the ligand susan^{Me}, we did not succeed in the synthesis of the analogous complex [(susan^{Me}){FeCl(μ-O)FeCl}]$^{2+}$ using the established protocol for the susan complex or by many variations of the reaction conditions. It should be noted, that the synthesis of

Stephan Walleck studied chemistry at Bielefeld University. He obtained his diploma in Chemistry in 2007 working on biomimetic diiron complexes with Prof. Thorsten Glaser. In 2010 he received his Ph.D. and got a permanent position as a scientific coworker of Prof. Thorsten Glaser. Currently he is working on the reactivity of dimetallic biomimetic complexes and on mixed-valence hetero- and homo-metallic pentanuclear complexes.

Thorsten Glaser studied chemistry in Bochum and obtained his Dr. rer. nat. in 1997 with Prof. K. Wieghardt at the Max-Planck-Institut, Mülheim. After postdoctoral work with Professors E. I. Solomon and K. O. Hodgson at Stanford University, he started his independent research in 2000 in Münster. Since 2005, he is full professor for inorganic chemistry at Bielefeld University. His research is focused on the rational design of functional transition metal complexes His current research projects are mainly in bioinorganic chemistry especially biomimetic oxidation catalysis and DNA recognition, in magnetochemistry especially single-molecule magnets and 2D monolayers, and in water oxidation catalysis.

Israel Journal of Chemistry

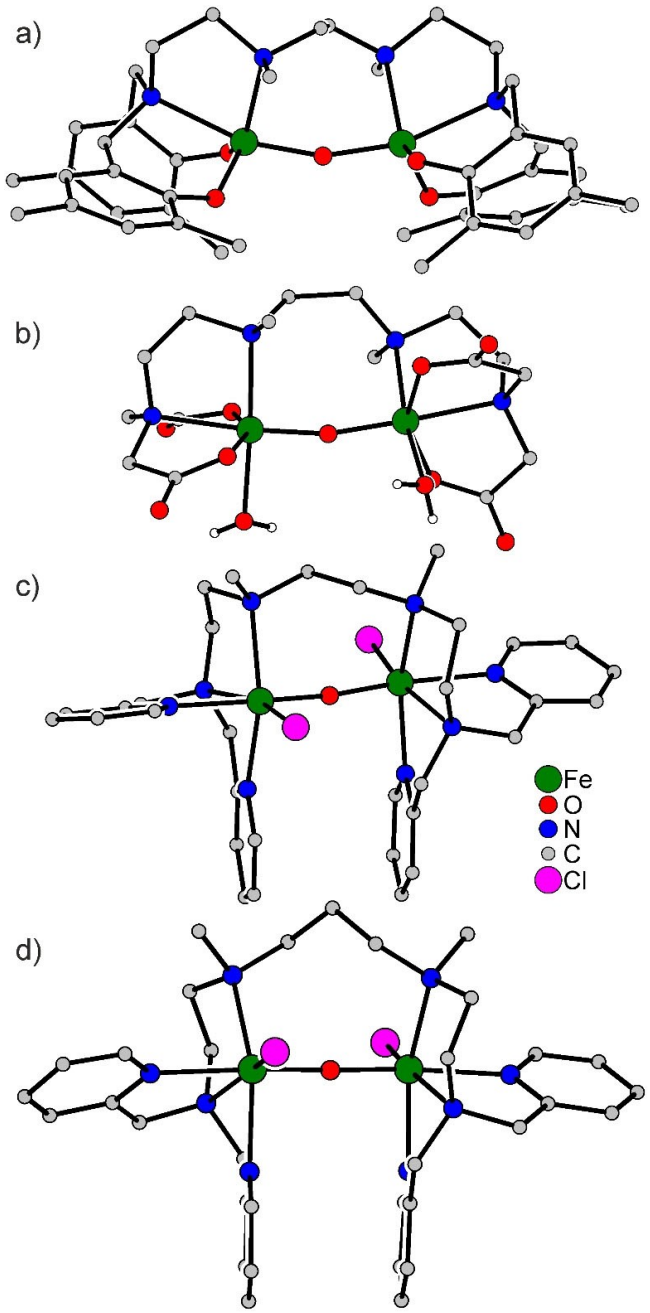

Figure 1. Molecular structures of a) [(hilde^{Me_2}){Fe(μ-O)Fe}], b) [(julia){Fe(OH$_2$)(μ-O)Fe(OH$_2$)}], c) [(susan){FeCl(μ-O)FeCl}]$^{2+}$, and d) [(susan^{Pr}){FeCl(μ-O)FeCl}]$^{2+}$.

[(susan){FeCl(μ-O)FeCl}]$^{2+}$ using the ligand susan and an Fe^{II} source in the presence of Cl$^-$ under basic aerobic conditions is simple enough to embed it in an undergraduate practical course. For a long period, we wondered for the reasons of this strong difference due to the introduction of a 6-methyl substituent (*vide infra*).

The coordination mode of the tetradentate ligand compartments differs in the two six-coordinate complexes [(julia){Fe(OH$_2$)(μ-O)Fe(OH$_2$)}] and [(susan){FeCl(μ-O)FeCl}]$^{2+}$. Due to their tripodal topology, both ligand compartments coordinate in a *cis* configuration but while the two terminal carboxylate donors of the ligand julia^{4-} are in a *trans* orientation, the two terminal pyridines of the ligand susan are in a *cis* orientation.[66] This wrapping of the ligand julia^{4-} causes an arrangement of the terminal H$_2$O ligands with a dihedral angle (H$_2$O–Fe–Fe–H$_2$O) of 59°. On the other hand, the two terminal Cl$^-$ donors in [(susan){FeCl(μ-O)FeCl}]$^{2+}$ are *trans* relative to the central Fe-μ-O–Fe core resulting in a dihedral angle of 170°.

The two coordination sites blocked by the Cl$^-$ ligands in [(susan){FeCl(μ-O)FeCl}]$^{2+}$ are intended as substrate binding sites during catalytic cycles. For a cooperative action of these two binding sites, they should preferably be in a *cis* configuration. The *trans* configuration in [(susan){FeCl(μ-O)FeCl}]$^{2+}$ is linked with a C_2 symmetric wrapping of the ligand susan around the {Fe^{III}(μ-O)Fe^{III}} core. The central ethylene spacer that connects the two ligand compartments exhibits a 'zig-zag' structure, which seems to enforce the C_2 symmetric ligand wrapping. We thought that the extension of this 'zig-zag' structure in the spacer by an additional CH$_2$ group, *i.e.* using a propylene spacer, should enforce a C_S symmetric wrapping of the ligand and hence a *cis* configuration of the two potential binding sites. In this respect, we used the analogue ligand susan^{Pr} with a central propylene instead of an ethylene spacer. This ligand susan^{Pr} was reported before by Schindler and coworkers for application in biomimetic copper chemistry.[67] We were able to obtain the intended complex [(susan^{Pr}){FeCl(μ-O)FeCl}](ClO$_4$)$_2$ (Figure 1d).[68] However, insertion of the third CH$_2$ group destroyed the 'zig-zag' structure. The central CH$_2$ groups points out from this chain sitting on the top providing again a C_S symmetric wrapping of the ligand and hence a *trans* configuration of the two chlorides (Figure 1d). This indicates that the central ethylene spacer introduced by tetramine **1** provides the appropriate distance for bridged dinuclear complexes while the propylene spacer in susan^{Pr} is too long requiring the propylene spacer to adopt an energetically more demanding arrangement.

As the active sites of the diiron metalloproteins are generally carboxylate-rich, we performed the reaction of susan and an Fe^{II} salt under basic atmospheric conditions also in the presence of an acetate source. Using 1 equiv. acetate results in the doubly-bridged complex [(susan){Fe(μ-O)(μ-OAc)Fe}](ClO$_4$)$_3$ (Figure 2a) and in the presence of 2 equiv. acetate in the μ-oxo-bridged complex [(susan){Fe(OAc)(μ-O)Fe(OAc)}](ClO$_4$)$_2$ (Figure 2b), whose molecular structure resembles that of [(susan){FeCl(μ-O)FeCl}](ClO$_4$)$_2$ with two terminally coordinated acetato ligands in *trans* configuration.[69,70] In [(susan){Fe(μ-O)(μ-OAc)Fe}]$^{3+}$, the bridging acetate binds to two *cis*-oriented coordination sites providing a first indication of the flexibility of this ligand system.

We put strong efforts to obtain a dinuclear doubly-bridged iron complex with the ligand susan with either a bis-μ-oxo (**F**), a μ-oxo,μ-hydroxo (**E**) or a bis-μ-hydroxo (**D**) core without success yet (Scheme 2). However, performing the standard

Israel Journal of Chemistry

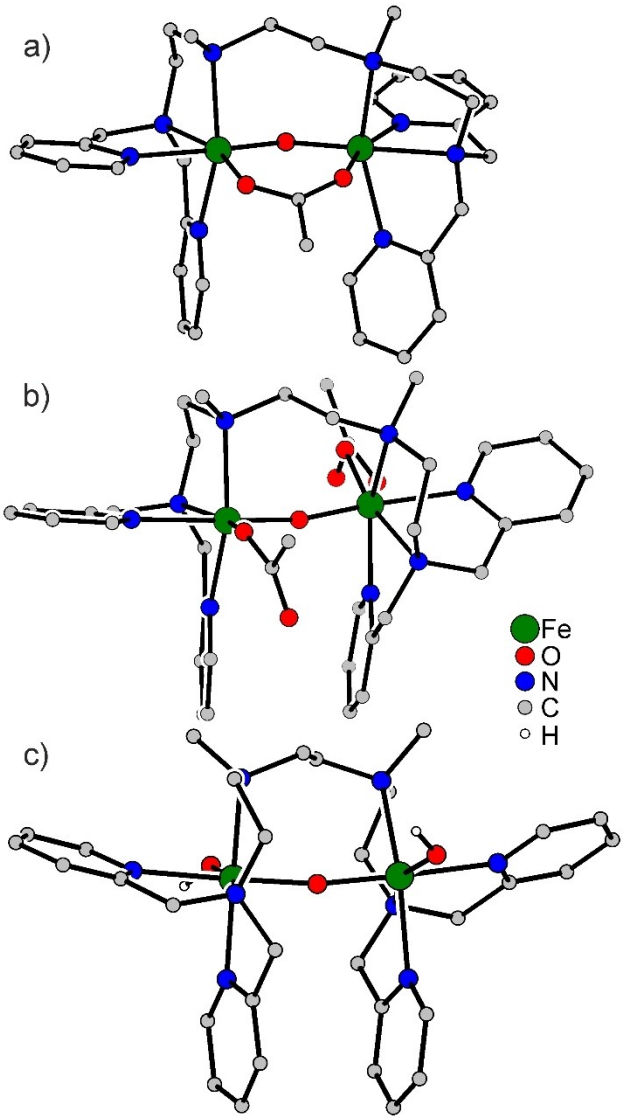

Figure 2. Molecular structures of $[(susan)\{Fe(\mu\text{-}O)(\mu\text{-}OAc)Fe\}]^{3+}$, $[(susan)\{Fe(OAc)(\mu\text{-}O)Fe(OAc)\}]^{2+}$, and $[(susan)\{Fe(OH)(\mu\text{-}O)Fe(OH)\}]^{2+}$.

protocol with an Fe^{II} salt and susan under basic aerobic conditions in a water/ethanol mixture without providing an exogenous anionic ligand results in the complex $[(susan)\{Fe(OH)(\mu\text{-}O)Fe(OH)\}](ClO_4)_2$, which contains two rare terminal hydroxo ligands (Figure 2c).[71] This accentuates the need in this series for a negatively charged exogenous ligand or in other words demonstrates the Lewis acidity of the $\{Fe^{III}(\mu\text{-}O)Fe^{III}\}$ core by using the ligand susan. This $\{Fe^{III}(OH)(\mu\text{-}O)Fe^{III}(OH)\}$ (**C** in Scheme 2) core is the hydrated form of the bis-μ-oxo $\{Fe^{III}(\mu\text{-}O)_2Fe^{III}\}$ core **F**.

In our efforts to obtain doubly-bridged complexes with oxo or hydroxo donors, we also employed $Fe^{II}(BF_4)_2\cdot 6H_2O$ as Fe^{II} source. Under aerobic basic conditions, using the ligand susan we obtained the mono-μ-oxo-bridged complex $[(susan)\{FeF(\mu\text{-}O)FeF\}](BF_4)_2$ with terminal fluoro ligands (Figure 3a)[72] indicating the hydrolysis of BF_4^-, which is a known reactivity.[73,74] Surprisingly, reacting $susan^{Me}$ with $Fe(BF_4)_2\cdot 6H_2O$ under the same aerobic conditions provided the

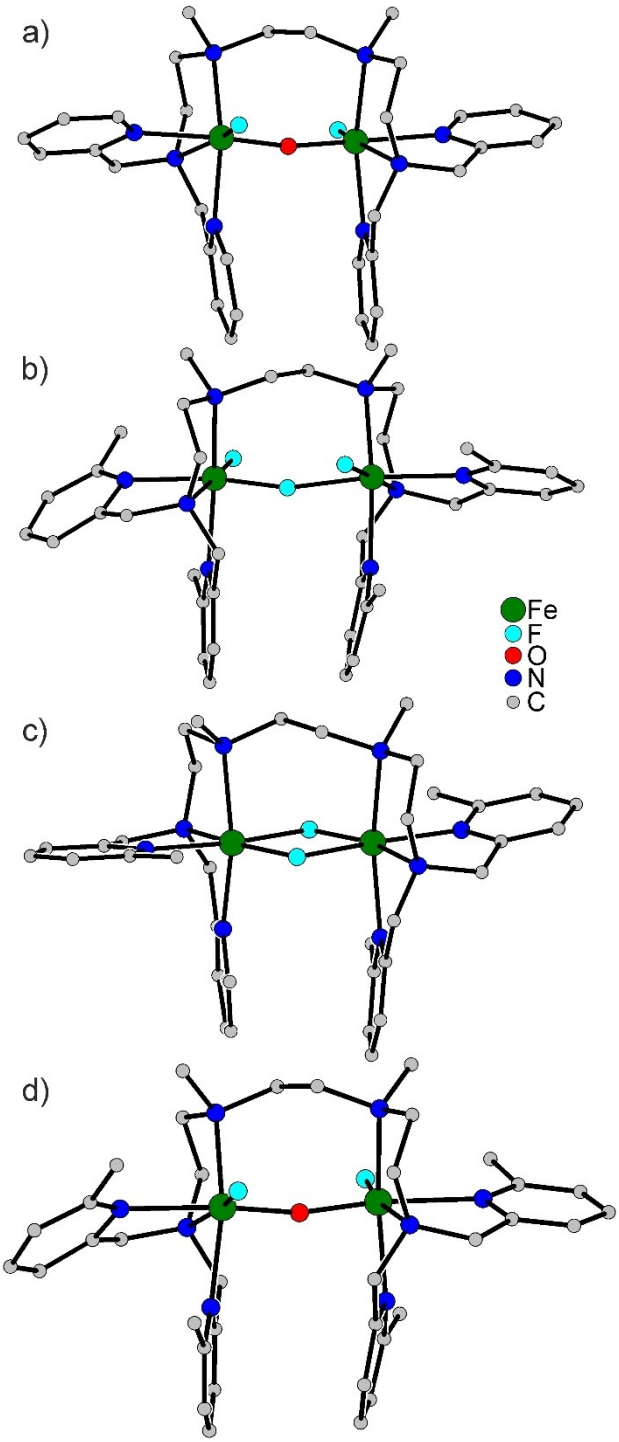

Figure 3. Molecular structures of a) $[(susan)\{FeF(\mu\text{-}O)FeF\}]^{2+}$, b) $[(susan^{Me})\{FeF(\mu\text{-}F)FeF\}]^{2+}$, c) $[(susan^{Me})\{Fe(\mu\text{-}F)_2Fe\}]^{2+}$, and d) $[(susan^{Me})\{FeF(\mu\text{-}O)FeF\}]^{2+}$.

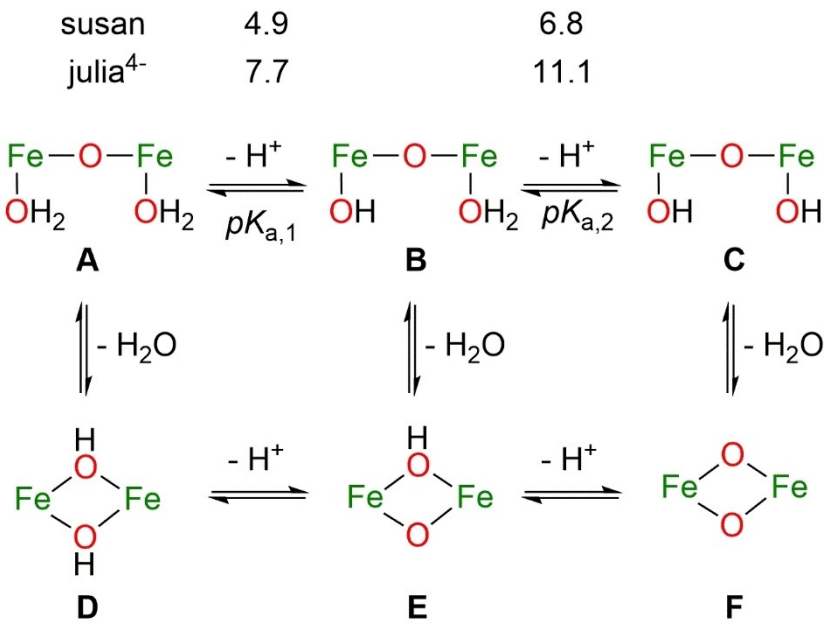

Scheme 2. Acid/base and condensation/hydration equilibria in μ-oxo-bridged diiron complexes.

μ-fluoro-bridged mixed-valent $Fe^{II}Fe^{III}$ complex $[(susan^{Me})\{Fe^{II}F(\mu\text{-}F)Fe^{III}F\}](BF_4)_2$ as the first iron complex of $susan^{Me}$ (Figure 3b).[48] Using anaerobic conditions, the bis-μ-fluoro-bridged $Fe^{II}Fe^{II}$ complex $[(susan^{Me})\{Fe(\mu\text{-}F)_2Fe\}](BF_4)_2$ was obtained (Figure 3c).[48]

These fluoro complexes demonstrated the principle accessibility of iron complexes with the ligand $susan^{Me}$. Therefore, we further intensed our efforts to obtain analogous μ-oxo-bridged complexes with $susan^{Me}$ using $Fe(BF_4)_2 \cdot 6H_2O$. As an $\{Fe^{III}(\mu\text{-}O)Fe^{III}\}$ complex could not be obtained under aerobic conditions, we added H_2O_2 to increase the oxidizing potential. Under these harsher conditions, we could indeed achieve the synthesis of the μ-oxo-bridged complex $[(susan^{Me})\{FeF(\mu\text{-}O)FeF\}](ClO_4)_2$ with terminal fluoro ligands (Figure 3d).[72] However, analogous complexes with terminal chloro or acetato ligands have still not been accessible with $susan^{Me}$ even under these harsher oxidizing conditions.

It is not straightforward that the introduction of a simple 6-methyl substituent in the pyridine donor causes such strong chemical differences. The introduction of the 6-methyl group should increase the electron density in the pyridine donor due to the $+I$ effect. This should strengthen the σ-donor ability of the pyridine and therefore strengthen and shorten the $Fe\text{–}N^{Py}$ bond. However, it was known, that $M\text{–}N^{Py}$ are longer for 6-methyl pyridine donors than for pyridine donors without substituents in the 6-position.[49,75–81] For iron complexes with tpa-based ligands an explanation was provided by a short distance of 2.7 Å of a hydrogen of the 6-methyl group to the iron ion.[81]

To obtain further insight we performed a systematic analysis of molecular structures exhibiting M–py units in the Cambridge Structural Database.[72] This provided, that the statement that $M\text{–}N^{py}$ bonds with 6-methyl pyridyl donors are always longer than the analogous complexes with unsubstituted pyridyl donors is only valid for six-coordinate complexes.[79,82,83] In five- or four-coordinate complexes, the difference in the $M\text{–}N^{py}$ bond lengths for 6-methyl pyridine and pyridine donors is mostly not significant. In a closer look, it turned out that longer $M\text{–}N^{py}$ of 6-methyl pyridine donors occur when the methyl group is pointing to a *cis*-coordinated ligand with an approximate 90° degree angle to the 6-methyl pyridine donor. This arrangement can also be observed in some five-coordinate complexes but is always the case in six-coordinate octahedral complexes. We therefore concluded that a steric repulsion between the 6-methyl substituent and the ligand in *cis* position in octahedral coordination elongates $M\text{–}N^{py}$ bonds for 6-methyl substituted pyridine donors.[72]

Indeed, this was manifested by comparing the molecular structures of the two μ-oxo-complexes $[(susan)\{FeF(\mu\text{-}O)FeF\}]^{2+}$ and $[(susan^{Me})\{FeF(\mu\text{-}O)FeF\}]^{2+}$ with terminal fluoro donors (Figure 4). It can be seen, that there is an overlap in $[(susan^{Me})\{FeF(\mu\text{-}F)FeF\}]^{2+}$ of the 6-methyl group with the fluoro ligand coordinated *cis* indicating strong steric repulsion, which is almost absent in $[(susan)\{FeF(\mu\text{-}O)FeF\}]^{2+}$.[72] This suggests, that the small F^- ligand is the only ligand, which can be enforced to coordinate *cis* to the 6-methyl pyridine by favoring the $Fe^{III}Fe^{III}$ state with H_2O_2 addition. However, larger ligands as Cl^- or OAc^- cannot coordinate with a 90° angle to a 6-methyl pyridine group.

Israel Journal of Chemistry

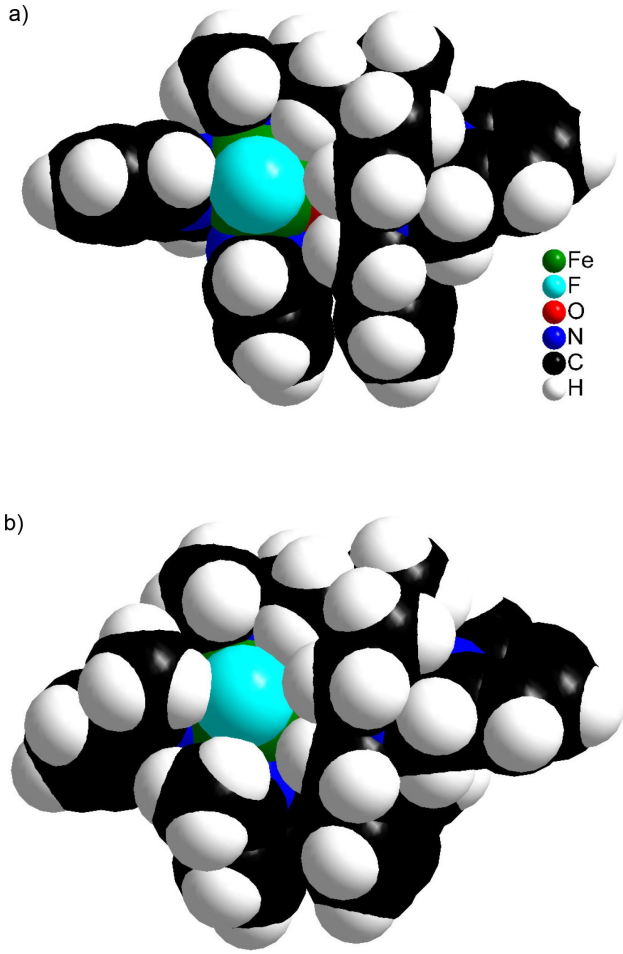

Figure 4. Space filling models of a) $[(susan)\{FeF(\mu\text{-}O)FeF\}]^{2+}$ and b) $[(susan^{Me})\{FeF(\mu\text{-}O)FeF\}]^{2+}$ illustrating the sterical hinderence of the 6-Me group with the fluoro donor bound in a 90° angle which is almost absent in the pure pyridine version $[(susan)\{FeF(\mu\text{-}O)FeF\}]^{2+}$.

4. A pH-Driven Reversible Carboxylate-Shift Observed in Solution at Room-Temperature

We studied the μ-oxo-bridged diiron complexes intensively by magnetic, electrochemical, and spectroscopic means.[45,66,69–71] It turned out, that the UV-Vis-NIR spectroscopic and magnetic properties are only slightly depending on the nature of the anionic ligand X^- in the mono-μ-oxo-bridged complexes $[(susan)\{Fe^{III}X(\mu\text{-}O)Fe^{III}X\}]^{2+}$.[66] However, the variation of the bridging mode from mono-bridged μ-oxo to doubly-bridged μ-oxo,μ-carboxylato results in strong differences in the UV-Vis-NIR spectra, which is known from tpa-based complexes.[84–86] Figure 5 shows a comparison of the UV-Vis-NIR spectra of the mono- $[(susan)\{Fe(OAc)(\mu\text{-}O)Fe(OAc)\}]^{2+}$ and doubly-bridged $[(susan)\{Fe(\mu\text{-}O)(\mu\text{-}OAc)Fe\}]^{3+}$ complexes.[69] The doubly-bridged nature in $[(susan)\{Fe(\mu\text{-}O)(\mu\text{-}OAc)Fe\}](ClO_4)_3$ results in prominent absorptions around 14000 and 20000 cm^{-1}, while only one weak band at

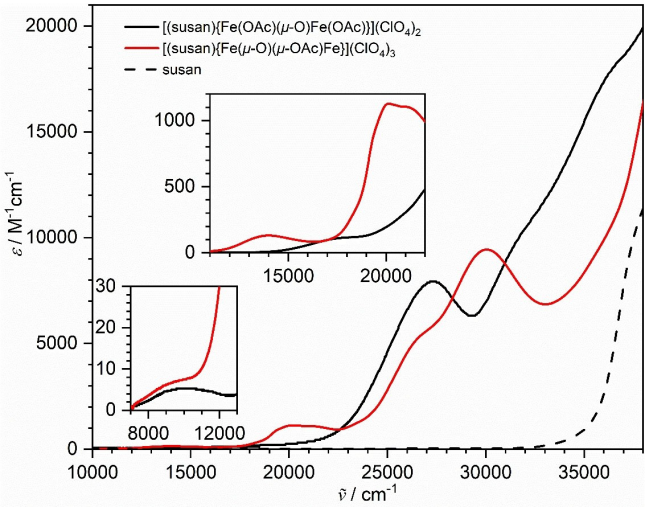

Figure 5. UV-Vis-NIR absorption spectra of $[(susan)\{Fe(\mu\text{-}O)(\mu\text{-}OAc)Fe\}]^{3+}$ and $[(susan)\{Fe(OAc)(\mu\text{-}O)Fe(OAc)\}]^{2+}$.

17000 cm^{-1} is characteristic for $[(susan)\{Fe(OAc)(\mu\text{-}O)Fe(OAc)\}]^{2+}$. Moreover, the strong μ-oxo→Fe^{III} LMCT is shifted from 27300 cm^{-1} in the mono-bridged complex to 30000 cm^{-1} in the doubly-bridged complex. In the vibronic spectra,[69] the terminal acetates in $[(susan)\{Fe(OAc)(\mu\text{-}O)Fe(OAc)\}]^{2+}$ are characterized by intense bands for the $\nu_{asym}(CO_2^-)$ and $\nu_{sym}(CO_2^-)$ stretching modes at 1639 cm^{-1} and 1372 cm^{-1}, respectively, while $[(susan)\{Fe(\mu\text{-}O)(\mu\text{-}OAc)Fe\}]^{3+}$ exhibits these two bands at 1535 and 1439 cm^{-1}. The ν_{asym}(Fe–O–Fe) mode shifts from 814 cm^{-1} in $[(susan)\{Fe(OAc)(\mu\text{-}O)Fe(OAc)\}]^{2+}$ to 764 cm^{-1} in $[(susan)\{Fe(\mu\text{-}O)(\mu\text{-}OAc)Fe\}]^{3+}$. These two spectroscopic methods provide thus useful signatures for the molecular structures not only in the solid state but also in solution.

In this respect, we have identified a reversible carboxylate shift in solution at room temperature by using these two spectroscopic methods.[69] Consecutive additions of $HClO_4$ and NEt_3 to a solution of $[(susan)\{Fe(OAc)(\mu\text{-}O)Fe(OAc)\}]^{2+}$ in MeCN (Figure 6a) produces the spectral signature of $[(susan)\{Fe(\mu\text{-}O)(\mu\text{-}OAc)Fe\}]^{3+}$ (14000 and 20000 cm^{-1}) and of $[(susan)\{Fe(OAc)(\mu\text{-}O)Fe(OAc)\}]^{2+}$ (17000 cm^{-1}), respectively. The time traces at selected wavenumbers of this reaction sequence (Figure 6b) show that addition of more than 1 equiv. NEt_3 or $HClO_4$ has no effect and that excess acid or base can be neutralized. This carboxylate shift can also be observed in solution by ATR FTIR (Figure 6c). Addition of 1 equiv. $HClO_4$ to $[(susan)\{Fe(OAc)(\mu\text{-}O)Fe(OAc)\}]^{2+}$ results in a spectrum that coincides with that of $[(susan)\{Fe(\mu\text{-}O)(\mu\text{-}OAc)Fe\}]^{3+}$. Addition of NEt_3 restores the spectrum of $[(susan)\{Fe(OAc)(\mu\text{-}O)Fe(OAc)\}]^{2+}$.

These data clearly demonstrate a reversible reaction between $[(susan)\{Fe(OAc)(\mu\text{-}O)Fe(OAc)\}]^{2+}$ and one H^+ to $[(susan)\{Fe(\mu\text{-}O)(\mu\text{-}OAc)Fe\}]^{3+}$. This indicates that a terminal acetate becomes protonated (Scheme 3). This protonation of a terminal acetate enables the substitution of the protonated

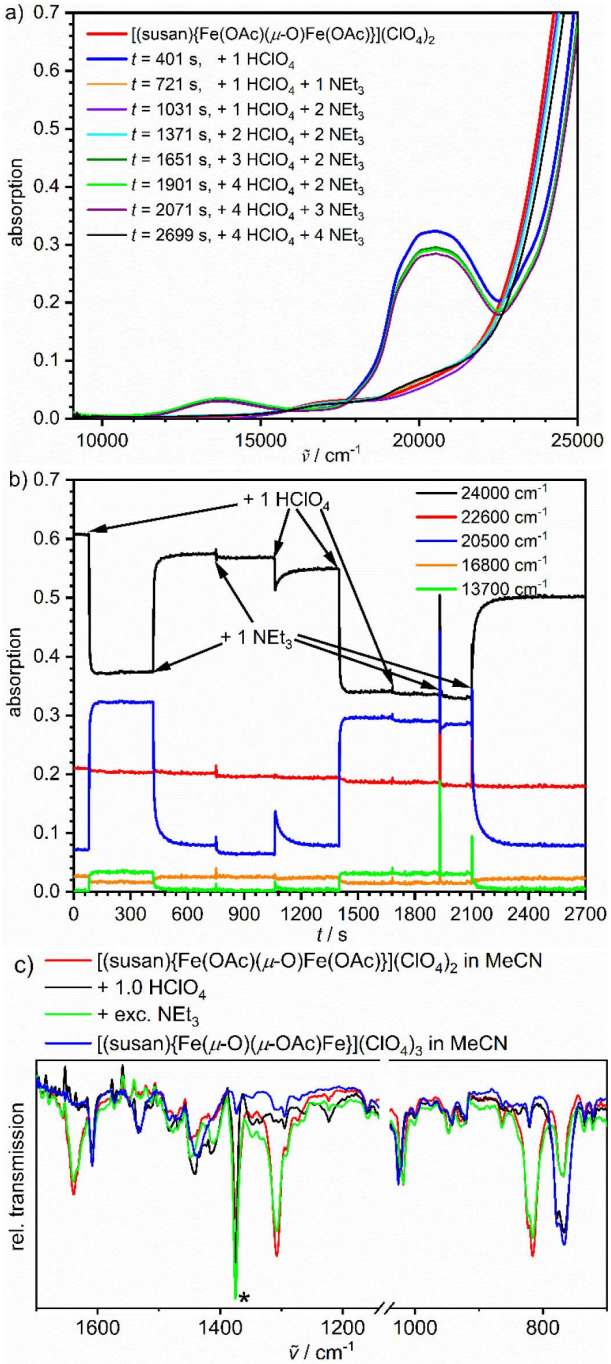

Figure 6. A reversible carboxylate shift triggered by acid/base additions in MeCN observed by UV-Vis-NIR (a and b) and FTIR (c) spectroscopies. a) UV-Vis-NIR spectra of [(susan){Fe(OAc)(μ-O)Fe(OAc)}]$^{2+}$ in MeCN solution upon subsequent $HClO_4$ and NEt_3 additions. Note that the equivalents provided in the figure are the total equivalents added. b) Time traces at selected wavenumbers for the spectra in a). c) ATR FTIR spectra of [(susan){Fe(OAc)(μ-O)Fe(OAc)}]$^{2+}$ in MeCN solution and after addition of $HClO_4$ and NEt_3. The spectrum after addition of $HClO_4$ coincides with that of [(susan){Fe(μ-O)(μ-OAc)Fe}]$^{3+}$. Addition of NEt_3 restores that of [(susan){Fe(OAc)(μ-O)Fe(OAc)}]$^{2+}$. The bands marked by * are from residual solvent absorptions. Reprinted with permission from reference [69]. Copyright 2018 American Chemical Society.

acetate by the other non-protonated acetate, which becomes bridging. This bridging acetate does not react with another H^+. However, adding one NEt_3 opens the acetate bridge. Based on the synthetic conditions it can be concluded that the protonated acetate becomes deprotonated and this nucleophilic acetate is then able to bind to a Fe^{III} ion substituting the bridging acetate.

5. Dependence of the pK_a Values of Coordinated H_2O Ligands by the Terminal Ligands

As protonation/deprotonation steps or proton-coupled electron-transfer steps play important roles in the mechanisms of metalloenzymes,[2,12,21,58,87–89] we investigated the complexes with terminal water-based ligands, *i.e.* [(julia){Fe(OH$_2$)(μ-O)Fe(OH$_2$)}] and [(susan){Fe(OH)(μ-O)Fe(OH)}]$^{2+}$, with respect to their pH-dependent behavior. First, their structural integrity in solution had to be proven to exclude variations during dissolution.

The 80 K ^{57}Fe Mössbauer spectrum of solid [(julia){Fe(OH$_2$)(μ-O)Fe(OH$_2$)}] shows a single quadrupole doublet ($\delta = 0.47$ mm s^{-1}, $|\Delta E_Q| = 2.04$ mm s^{-1}).[45,46] Frozen aqueous solutions at 80 K of a ^{57}Fe–enriched sample at pH = 5.93 reveals only minor changes to the solid state ($\delta = 0.47$ mm s^{-1}, $|\Delta E_Q| = 1.97$ mm s^{-1}). On the other hand, the substitution of the H_2O ligands by DMSO ligands, *i.e.* [(julia){Fe(DMSO)(μ-O)Fe(DMSO)}], changes the solid-state Mössbauer spectrum more strongly ($\delta = 0.47$ mm s^{-1}, $|\Delta E_Q| = 1.91$ mm s^{-1}) than dissolution in H_2O. This demonstrates the molecular integrity of [(julia){Fe(OH$_2$)(μ-O)Fe(OH$_2$)}] upon dissolution in H_2O.

The solid-state Mössbauer spectrum of [(susan){Fe(OH)(μ-O)Fe(OH)}](ClO$_4$)$_2$ reveals two quadrupole doublets ($\delta_1 = 0.45$ mm s^{-1}, $|\Delta E_Q|_1 = 2.00$ mm s^{-1}; $\delta_2 = 0.44$ mm s^{-1}, $|\Delta E_Q|_2 = 1.57$ mm s^{-1}). This difference originates from different kinds of hydrogen-bonding of the coordinated OH^- ligand in the solid-state structure. One coordinated OH^- acts as a hydrogen bond donor while the other acts as a hydrogen bond acceptor. This induces a 0.054 Å difference in the Fe^{III}–OH bond lengths, which in turn affects the quadrupole splitting.[71] The spectrum of a frozen MeCN solution shows a single quadrupole doublet ($\delta = 0.45$ mm s^{-1}, $|\Delta E_Q| = 1.71$ mm s^{-1}) close to the mean values of the solid-state spectrum indicating a more symmetrical second sphere in solution. The UV-Vis-NIR spectrum of [(susan){Fe(OH)(μ-O)Fe(OH)}]$^{2+}$ in MeCN solution shows the ligand-field transitions $^6A_1 \rightarrow {}^4T_1$ at 9840 cm^{-1} and $^6A_1 \rightarrow {}^4T_2$ at 17850 cm^{-1}, which remain almost unchanged in the solid-state reflectance spectrum.[71] As the UV-Vis-NIR spectra in H_2O (*vide infra*) and MeCN solutions are almost superimposable, these experiments demonstrate the molecular integrity of [(susan){Fe(OH)(μ-O)Fe(OH)}]$^{2+}$ upon dissolution in H_2O.

To obtain the pK_a values, we performed pH-dependent UV-Vis spectroscopies in aqueous solution by titration experiments and obtained two pK_a values for each complex: 4.9 and 6.8 for [(susan){Fe(OH)(μ-O)Fe(OH)}]$^{2+}$[45,46] and 7.7 and 11.1 for

Israel Journal of Chemistry

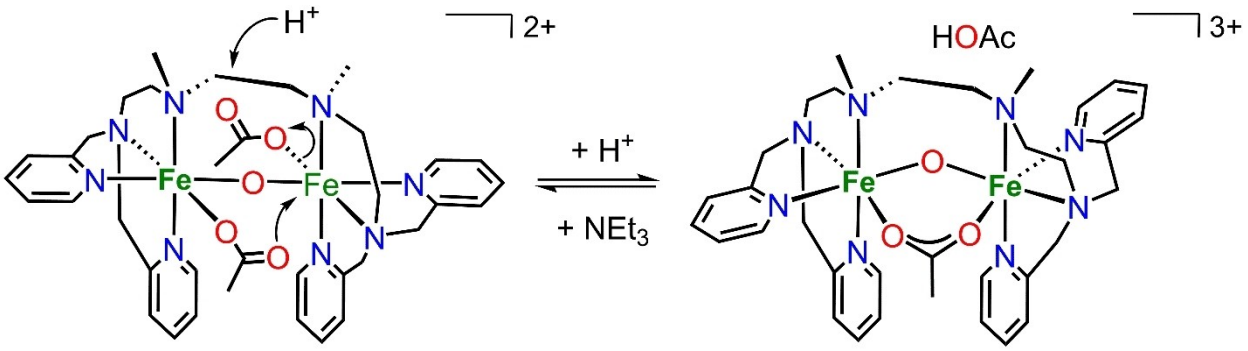

Scheme 3. Reversible carboxylate shift between [(susan){Fe(OAc)(μ-O)Fe(OAc)}]$^{2+}$ and [(susan){Fe(μ-O)(μ-OAc)Fe}]$^{3+}$ in MeCN solution.

[(julia){Fe(OH$_2$)(μ-O)Fe(OH$_2$)}].[71] Scheme 2 defines the acid/base equilibria. In this respect, [(julia){Fe(OH$_2$)(μ-O)Fe(OH$_2$)}] represents protonation state **A** and [(susan){Fe(OH)(μ-O)Fe(OH)}]$^{2+}$ protonation state **C**. In general, the various protonation states can also undergo condensation reactions (Scheme 2). The fully protonated form **A** with two terminal aqua ligands may be in equilibrium with its condensation product **D** with a bis-μ-hydroxo core.[45,86,90,91] The same holds true for the medium protonation state **B** with one terminal hydroxo ligand and one terminal aqua ligand, which can condense to a doubly-bridged μ-oxo,μ-hydroxo core **E**.[45,86,90] Furthermore, the fully deprotonated form can exist with two terminal hydroxo ligands (**C**) or with a bis-μ-oxo-bridged core **F**. All of these core motifs have examples in the literature with clearly distinct spectroscopic features of the mono-bridged μ-oxo complexes and the corresponding doubly-bridged condensation products.[86,92]

The UV-Vis-NIR spectrum of [(susan){Fe(OH)(μ-O)Fe(OH)}]$^{2+}$ in aqueous solution (pH = 9.8 in Figure 7a) exhibits the pyridine π→π* transition at 38800 cm^{-1}, two strong μ-oxo→Fe^{III} LMCT transitions at 28400 and 32200 cm^{-1} and a lower intensity LMCT around 20700 cm^{-1}. Even lower intense but well resolved LF transitions are observed at 17400 cm^{-1} ($^6A_1 \rightarrow {}^4T_2$) and 10000 cm^{-1} ($^6A_1 \rightarrow {}^4T_1$).[71] Mono- and doubly-protonation (Figure 7a) only slightly changes these features indicating the conservation of the mono-μ-oxo bridged structures, *i.e.* going from **C**→**B** and from **B**→**A**. Moreover, the absence of a pronounced band around 18000 cm^{-1}, which is a well-established signature for a doubly-bridged μ-oxo,μ-hydroxo core **E**,[86,93] should be interpretated as a criterion for exclusion of the doubly-bridged core structure. The mono-bridged μ-oxo complex **B** with a hydroxide ligand at one iron center and an aqua ligand at the other iron center is most likely stabilized by an intramolecular hydrogen bond, which is indicated by water exchange experiments.[71]

These assignments are further corroborated by spectroscopic characterizations at −40 °C in MeCN solutions. Addition of 1 or 2 equiv. of HClO$_4$ to [(susan){Fe(OH)(μ-O)Fe(OH)}]$^{2+}$ provides the medium-protonated form **B** and the fully protonated form **A**, respectively. UV-Vis-NIR spectroscopy on these MeCN solutions at −40 °C confirm the spectral changes observed on aqueous solutions. An interesting feature is the shift of the $^6A_1 \rightarrow {}^4T_2$ transition from 17850 cm^{-1} in

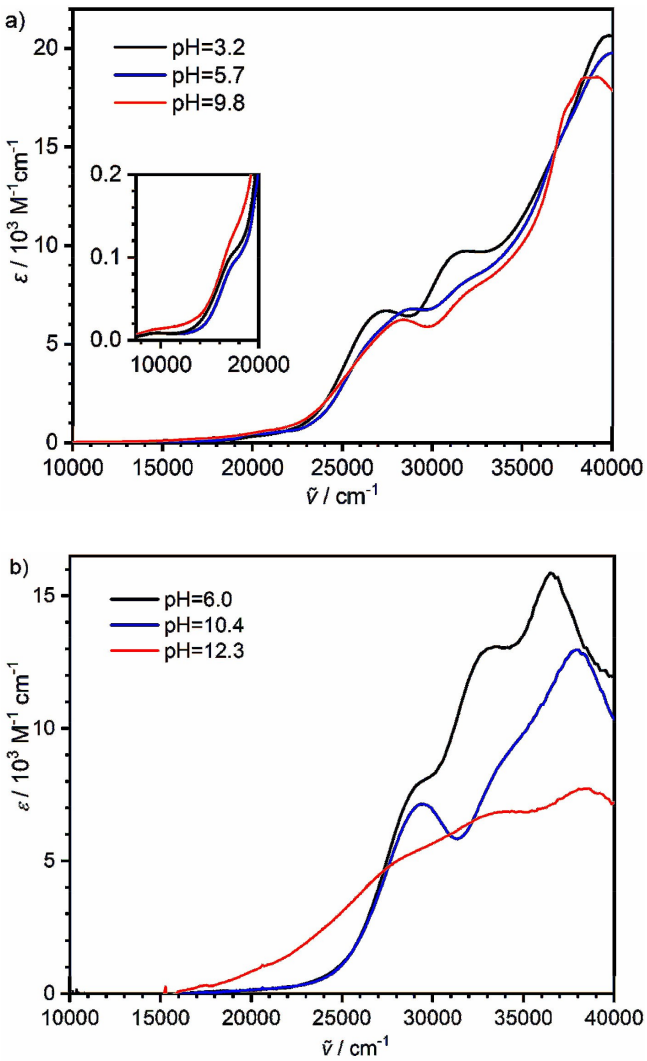

Figure 7. pH-Dependent UV-Vis-NIR spectra of a) [(susan){Fe(OH)(μ-O)Fe(OH)}]$^{2+}$ and b) [(julia){Fe(OH$_2$)(μ-O)Fe(OH$_2$)}] in H$_2$O.

[(susan){Fe(OH)(μ-O)Fe(OH)}]$^{2+}$ to lower energy at 16000 cm^{-1} in the fully protonated form **A**. Considering that the $^6A_1 \rightarrow {}^4T_1$ and $^6A_1 \rightarrow {}^4T_2$ transitions have negative slopes in the Tanabe-Sugano diagram, this shift to lower energy upon protonation indicates a stronger ligand field strength. The stronger ligand field in the protonated species accounts for lower π-donation of a H_2O ligand in comparison to a hydroxo ligand. Interestingly, the spectrum of the mono-protonated species exhibits both $^6A_1 \rightarrow {}^4T_2$ transitions at 17850 cm^{-1} and 16000 cm^{-1} in accordance to the presence of both a terminal water and a terminal hydroxo ligand.[71] The Mössbauer spectrum in MeCN is only slightly affected upon protonation: **C**, $\delta = 0.45$ mm s^{-1}, $|\Delta E_Q| = 1.71$ mm s^{-1}; **D**, $\delta = 0.46$ mm s^{-1}, $|\Delta E_Q| = 1.67$ mm s^{-1}; **A**, $\delta = 0.48$ mm s^{-1}, $|\Delta E_Q| = 1.62$ mm s^{-1}. All these spectroscopic data clearly indicate that all three protonation states of [(susan){Fe(OH)(μ-O)Fe(OH)}]$^{2+}$ are mono-brigded μ-oxo complexes.

The electronic absorption spectrum of an aqueous solution of [(julia){Fe(OH_2)(μ-O)Fe(OH_2)}] (Figure 7b, pH = 6.0) is dominated by intense absorption features above 25000 cm^{-1}. While the absorption at 36600 cm^{-1} has a strong carboxylate→Fe^{III} charge transfer character assigned by titration experiments, the bands at 28900 cm^{-1} and 32800 cm^{-1} are mainly of μ-oxo→Fe^{III} LMCT character close to the bands in [(susan){Fe(OH)(μ-O)Fe(OH)}]$^{2+}$.[45,46] Mono-deprotonation of [(julia){Fe(OH_2)(μ-O)Fe(OH_2)}] still shows the strong μ-oxo→Fe^{III} LMCT at 29500 cm^{-1} while the second LMCT decreases in intensity (Figure 7b) and no band around 18000 cm^{-1} is observed as signature for a doubly-bridged core **E**. The Mössbauer spectrum changes only slightly to $\delta = 0.47$ mm s^{-1} and $|\Delta E_Q| = 1.68$ mm s^{-1}, so that the mono-deprotonated form is assigned to **B**. Contrarily, a doubly-deprotonation results in strong variations as no resolved μ-oxo→Fe^{III} LMCT are observed and additional intensity is observed at lower energy (Figure 7b). Moreover, the Mössbauer parameters change to $\delta = 0.46$ mm s^{-1} and $|\Delta E_Q| = 0.70$ mm s^{-1}. These variations indicate a major reorganization, probably a condensation to the bis-μ-oxo core **F**.

The different pK_a values of [(julia){Fe(OH_2)(μ-O)Fe(OH_2)}] ($pK_{a,1} = 7.7$, $pK_{a,2} = 11.1$) and [(susan){Fe(OH)(μ-O)Fe(OH)}]$^{2+}$ ($pK_{a,1} = 4.9$, $pK_{a,2} = 6.8$) reflect the varying donation capabilities of the ligands. On the one hand, the ligand julia^{4-}, which mimics the carboxylate-rich coordination environments of non-heme diiron enzymes, exhibits four σ-donating carboxylato donors with further π-donation capabilities. The complex [(julia){Fe(OH_2)(μ-O)Fe(OH_2)}] of this ligand could only be isolated with two additional relatively weakly donating aqua donors. On the other hand, the four terminal pyridine donors of the ligand susan are σ-donors with no π-donation but with π-acceptor capabilities. This results in less electron-rich (more Lewis acidic) Fe^{III} ions in [(susan){Fe(OH)(μ-O)Fe(OH)}]$^{2+}$, which therefore prefer the strongly σ- and π-donating hydroxo ligands. Thus, the pK_a values obtained are more acidic. The four strong terminal σ- and π-donating phenolates in μ-oxo-bridged [(hilde^{Me_2}){Fe(μ-O)Fe}] induce highly covalent bonds to the Fe^{III} ions. Thus, the five-coordinate Fe^{III} ions are already electronically saturated without significant Lewis acidity even preventing the coordination of a sixth ligand.[45] Thus, the donation capabilities of the tetramine **1** based ligands decrease as (hilde^{Me_2})$^{4-}$ > (julia)$^{4-}$ > susan.

6. Influence of the Terminal and Exogenous Donors on Redox Potentials

[(hilde^{Me_2}){Fe(μ-O)Fe}] and the μ-oxo-bridged diferric complexes with our mononucleating analogues of H_4hilde^{Me_2} can be oxidized at relatively low potentials.[45,62,64,65] Spectroscopic characterizations of the oxidized species reveal, that the oxidations are ligand-centered leading to mono- and di-phenoxyl radical complexes.[62,65] The latter accumulating the same number of oxidation equivalents as intermediate **Q** from sMMO. In contrast to the phenolate containing ligands, the ligands julia^{4-} and susan are redox-innocent and in consequence oxidative processes should be metal-centered.[45,46]

The electrochemical characterization of the μ-oxo-bridged diferric complexes of the ligand susan [(susan){Fe^{III}X(μ-O)Fe^{III}X}]$^{2+}$ reveal irreversible oxidation processes.[45,70,71] The peak potential in V *vs* Fc^+/Fc of these oxidations span a large range depending on the exogenous ligand X: Cl^- 1.48, OAc^- 1.45, F^- 1.40, OMe^- 1.14, and OH^- 0.79. It is interesting that in such an isostructural series the variation of only one ligand can influence this redox potential so strongly. This variation demonstrates the different electron-density donation ability of the exogenous ligands.[45,46,70,71] Remarkable is the strong cathodic shift of 690 mV by substituting Cl^- by OH^-, which implies a strong stabilization of Fe^{IV} by the strongly σ- and π-donating hydroxo ligand.

Going from [(susan){Fe(OAc)(μ-O)Fe(OAc)}]$^{2+}$ to [(susan){Fe(μ-O)(μ-OAc)Fe}]$^{3+}$ results in an anodic shift out of the potential window of our experiment.[70] This strong shift is mainly attributed to the change of the overall charge from 2+ to 3+. According to the Born equation, an increase (decrease) of the total charge increases (decreases) redox potentials.[94,95]

The electrochemistry of [(julia){Fe(OH_2)(μ-O)Fe(OH_2)}] in H_2O shows no oxidation but only two metal-centered reductions with peak potentials at −0.25 and −0.56 V *vs* SHE. The CV of the mono-deprotonated species exhibits one reduction with a peak potential at −0.92 V *vs* SHE. In accordance with the core structure **B**, this reduction should be associated with the Fe^{III} coordinated to the remaining H_2O ligand. The shift to lower potential is again explained by the Born equation due to the decrease of the overall charge (0 in **A**, −1 in **B**). Remarkably, the doubly-deprotonation of [(julia){Fe(OH_2)(μ-O)Fe(OH_2)}] results in a quasi-reversible wave at −0.75 V *vs* SHE. A reduction should be shifted even further cathodically by the second protonation caused by the decrease of the overall charge from −1 to −2 in respect to Born's equation.[95] This conflicting observation coincides with the structural change to the bis-μ-oxo core **F**. Therefore, this redox

wave is attributed to a metal-centered oxidation of the diferric complex of core **F**. This very low potential for oxidation to a $Fe^{IV}Fe^{III}$ species is attributed to the overall −2 charge (Born equation) in combination with the strongly electron donating bis-μ-oxo core **F** and the terminal donor set of julia^{4-}.[46]

7. A High-Valent $Fe^{III}Fe^{IV}$ Complex of Ligand julia^{4-}

As described above, the doubly-deprotonation of [(julia){Fe(OH_2)(μ-O)Fe(OH_2)}] generates the dianionic complex [(julia){Fe^{III}(μ-O)$_2$$Fe^{III}$}]$^{2-}$ with a low-lying quasi-reversible potential for the metal-centered oxidation of the diferric complex at −0.75 *vs* SHE. This low-lying potential makes the oxidation feasible for dissolved molecular oxygen as oxidant. In this respect, a simple deprotonation experiment of [(julia){Fe(OH_2)(μ-O)Fe(OH_2)}] (pH = 13.0) performed under aerobic conditions leads to an axial $S_t = 1/2$ EPR spectrum with $g_{II} = 2.0982$ and $g_I = 2.0066$ and a spin concentration of 0.24 %.[46] Based on the concentration of dissolved oxygen saturated in water the spin concentration corresponds to a yield for oxidation of 4.4 %.[46] The analogous experiment under strict exclusion of O_2 provided an EPR-silent sample.

As no homo-valence $Fe^{III}Fe^{III}$ species can be accounted for this signal, it must arise from an oxidized or a reduced mixed valence species. The strong anisotropy of the EPR spectrum clearly demonstrate a metal-centered redox process. Taking into account the low-lying potential for the oxidation of the twofold deprotonated species, an oxidation of the diferric complex by dissolved O_2 is highly likely. This assignment is proved by spin projection analysis. While an isotropic $g_i = 2.00$ is a good approximation for any Fe^{III} h.s. component, Fe^{II} h.s. has $g_i > 2.0$ and Fe^{IV} h.s. $g_i < 0$. As the $S_i = 2$ component (either Fe^{IV} h.s. or Fe^{II} h.s) has in both scenarios to be antiparallel to the total $S_t = {}^1/_2$ spin ground state, spin projection rules out the Fe^{II} h.s. scenario which must result in a $g_{av} < 2.0$.[96] On the other hand the observed axial $S_t = 1/2$ spectrum with $g_{av} > 2.0$ is in agreement with an antiferromagnetic coupled Fe^{III} h.s.–Fe^{IV} h.s. spin system.

The extraordinary donation capabilities of the coordination environment in [(julia){Fe^{III}(μ-O)$_2$$Fe^{III}$}]$^{2-}$ makes the Fe^{III} ions very electron rich. Positively speaking, this high electron density is the origin of the low potential for oxidation. On the other hand, this high electron density in combination with the high pH values needed for generation of the doubly-deprotonated complex causes a limited stability resulting in a decoordination of the ligand julia^{4-} and formation of rust. The usual stabilization by cooling the solution is prevented by the solubility in H_2O and the insolubility in organic solvents.

8. Summary and Outlook

To mimic dinuclear active sites of metalloproteins, we have developed a dinucleating ligand system with varying terminal donors. Two tripodal ligand compartments are covalently linked by a flexible ethylene spacer providing the ligands (julia)$^{4-}$ with terminal carboxylates, (hilde^{Me_2})$^{4-}$ with terminal phenolates, and susan/susan^{Me} with terminal pyridines. These ligands provide access to a series of complexes with a {Fe^{III}(μ-O)Fe^{III}} core. A central propylene instead of the ethylene spacer seems to be too long requiring an energetically less favorable conformation of the propylene unit. The differences in the electron donation properties of the terminal ligands strongly vary the Lewis acidity of the {Fe^{III}(μ-O)Fe^{III}} core evidenced by only five-coordinate in [(hilde^{Me_2}){Fe(μ-O)Fe}] but six-coordinate in [(julia){Fe(OH_2)(μ-O)Fe(OH_2)}] and [(susan){FeX(μ-O)FeX}]$^{2+}$. Moreover, in the six-coordinate complexes the stronger electron donating character of the carboxylates of (julia)$^{4-}$ requires only neutral exogenous ligands while the lower electron donation of the pyridines of susan requires negatively charged ligands to saturate the higher Lewis acidity. This provides even the easy access to terminal OH^- ligands, which are very rare in Fe^{III} chemistry. Thus, the electron donation capabilities decrease in the order (hilde^{Me_2})$^{4-}$ > (julia)$^{4-}$ > susan. The different Lewis acidity of the {Fe^{III}(μ-O)Fe^{III}} core is quantified by the variation of the Brönstedt acidity of the coordinated H_2O/OH^- ligands. The more acidic pK_a values of [(susan){Fe(OH)(μ-O)Fe(OH)}]$^{2+}$ (4.9 and 6.8) resemble the higher Lewis acidity of its {Fe^{III}(μ-O)Fe^{III}} core than that of [(julia){Fe(OH_2)(μ-O)Fe(OH_2)}] (7.7 and 11.1) because it requires lower pH values to protonate the coordinated OH^- ligands and thus reducing its donation capabilities.

The intensive spectroscopic characterization of this series of complexes provided spectroscopic signatures of the molecular structures. This allows to use UV-Vis-NIR, FTIR, and Mössbauer spectroscopies to even evaluate the molecular structures in solution. A pH-dependent study showed that the differently protonated species of [(susan){Fe(OH)(μ-O)Fe(OH)}]$^{2+}$ and [(julia){Fe(OH_2)(μ-O)Fe(OH_2)}] have a mono-bridged {Fe^{III}(μ-O)Fe^{III}} core except the fully deprotonated form of (julia)$^{4-}$, whose molecular structure seems to be the bis-μ-oxo species [(julia){Fe^{III}(μ-O)$_2$$Fe^{III}$}]$^{2-}$.

This opportunity to evaluate molecular structures in solution also made it possible to observe a reversible carboxylate-shift between [(susan){Fe(OAc)(μ-O)Fe(OAc)}]$^{2+}$ and [(susan){Fe(μ-O)(μ-OAc)Fe}]$^{3+}$ triggered by successive acid/base additions. This carboxylate-shift requires a rearrangement of at least one ligand compartment (Scheme 3) providing an additional indication on the flexibility of these dinucleating ligands. As it is clearly visible from the time traces in Figure 6b, these reactions are on a second time scale indicating that eventually necessary rearrangements during catalytic cycles are possible on fast times scales. This reversible carboxylate shift also provides mechanistic scenarios for enzyme reactivities:

(*i*) a H^+ can open a coordination site for substrate binding at a terminal carboxylate but not at a bridging carboxylate and

(*ii*) a nucleophilic substrate can bind to a Fe^{III} center by substituting a bridging carboxylate.

The electrochemical analyses of all these complexes provide a strong influence of the terminal and of the exogenous ligands on the potentials for oxidation. Complexes with terminal phenolates as in [(hilde^{Me_2}){Fe(μ-O)Fe}] or in our analogous mononucleating ligands are not metal- but ligand-centered oxidized resulting in mono- and di-phenoxylradical complexes. On the other hand, coordinated carboxylates and pyridines are considered redox-inert for oxidations so that it is most likely that the complexes of (julia)$^{4-}$ and susan/susan^{Me} will be metal-centered oxidized. In the series [(susan){FeX(μ-O)FeX}]$^{2+}$ with X = Cl^-, F^-, OAc^-, OMe^-, and OH^-, the sole variation of the exogenous ligands strongly tunes the potential for the irreversible oxidation with the strongly σ- and π-donating OH^- ligand facilitating oxidation to Fe^{IV} by 690 mV in comparison to Cl^-.

The complex of [(julia){Fe(OH_2)(μ-O)Fe(OH_2)}] is only soluble in H_2O without substitution of the exogenous H_2O ligand. Solution measurements are hence only possible in the biologically most relevant solvent H_2O but this prevents stabilization of reactive species by experiments at low temperatures. The doubly-deprotonation of [(julia){Fe(OH_2)(μ-O)Fe(OH_2)}] results in a structural reorganization, which most probably results in the bis-μ-oxo core [(julia){Fe^{III}(μ-O)$_2$ Fe^{III}}]$^{2-}$. This structural reorganization is correlated with and thus corroborated by a change of the electrochemical properties in H_2O. The neutral and mono-anionic form with both of a mono-μ-oxo core exhibit no special redox wave. In contrast, the doubly-deprotonated species exhibits a very low potential for oxidation at -0.75 V *vs* SHE. This can be assigned to the combination of the dianionic charge and the strongly electron donating coordination environment of not only the terminal carboxylates but also the two bridging oxo ligands. This low potential for oxidation results in the oxidation at room temperature even by dissolved O_2 to [(julia){Fe^{IV}h.s.(μ-O)$_2$ Fe^{III}h.s}]$^-$ with a $S_t = {}^1/_2$ ground state with an axial EPR spectrum of $g_{av} > 2$. This room-temperature aqueous-solution oxidation by O_2 shows the potential of these dinucleating ligands for stabilizing high-valent species.

A quite difficult to understand observation was that the introduction of 6-methyl-substituents to the pyridines (going from susan to susan^{Me}) prevents the synthesis of complexes with a {Fe^{III}(μ-O)Fe^{III}} core, which is straightforward with susan. Only fluoro-bridged diferrous [(susan^{Me}){Fe^{II}(μ-F)$_2$ Fe^{II}}]$^{2+}$ and mixed valence [(susan^{Me}){Fe^{III}(μ-F)$_2$$Fe^{II}$}]$^{2+}$ were obtained in the presence of BF_4^-. Only by enforcing the oxidative conditions with excess H_2O_2, the μ-oxo diferric [(susan^{Me}){Fe^{III}F(μ-O)Fe^{III}F}]$^{2+}$ could be synthesized. Comparison of its structure to [(susan){Fe^{III}F(μ-O)Fe^{III}F}]$^{2+}$ and a CSD search provides the steric repulsion between the 6-methyl-group and the ligand in *cis* position in octahedral complexes as origin for the known longer M-N^{py} bonds of 6-methyl pyridines than of pyridines without a 6-substituent. Only the smallest ligand F^- fits in this pocket while all other ligands do not.

However, the straightforward syntheses of μ-oxo-bridged complexes [(susan){Fe^{III}X(μ-O)Fe^{III}X}]$^{2+}$ with varying terminal donors X^- even OH^- can also be interpreted as a thermodynamic preference for this structural motive. In contrast, the steric repulsion of X^- with the 6-methyl substituents should makes this molecular structure thermodynamically less favorable for the ligand susan^{Me}.[48] As a consequence, this could provide the opportunity that doubly-bridged complexes **D**, **E**, or **F** (Scheme 2) are the thermodynamically preferred structures with the ligand susan^{Me}.[71] Indeed, inspired by this interpretation we employ in our current efforts the ligand susan^{Me} to obtain doubly-bridged structures and were very recently successful in the crystallization of a stable μ-oxo,μ-peroxo complex of the ligand susan^{Me}.[97] The spectroscopic signatures of this peroxo complex allows us on the other hand to identify the analogous peroxo complex of the ligand susan as an unstable intermediate during catalytic processes. This peroxo complex converts to an even less stable high-valent intermediate that oxidizes C–H bonds.[98]

Acknowledgements

Open access funding enabled and organized by Projekt DEAL.

References

[1] L. Que Jr., A. E. True, *Prog. Inorg. Chem.* **1990**, *38*, 97–200.
[2] E. I. Solomon, T. C. Brunold, M. I. Davis, J. N. Kemsley, S.-K. Lee, N. Lehnert, F. Neese, A. J. Skulan, Y.-S. Yang, J. Zhou, *Chem. Rev.* **2000**, *100*, 235–349.
[3] A. J. Jasniewski, L. Que, *Chem. Rev.* **2018**, *118*, 2554–2592.
[4] M. A. Holmes, I. Le Trong, S. Turley, L. C. Sieker, R. E. Stenkamp, *J. Mol. Biol.* **1991**, *218*, 583–593.
[5] A. K. Shiemke, T. M. Loehr, J. Sanders-Loehr, *J. Am. Chem. Soc.* **1986**, *108*, 2437–2443.
[6] R. E. Stenkamp, *Chem. Rev.* **1994**, *94*, 715–726.
[7] D. T. Logan, X.-D. Su, A. Aberg, K. Regnstrom, J. Hadju, H. Eklund, P. Nordlund, *Structure* **1996**, *4*, 1053–1064.
[8] P. Nordlund, B.-M. Sjöberg, H. Eklund, *Nature* **1990**, *345*, 393–398.
[9] K. E. Liu, A. M. Valentine, D. Wang, B. H. Huynh, D. E. Edmondson, A. Salifoglou, J. Lippard, *J. Am. Chem. Soc.* **1995**, *117*, 10174–10185.
[10] S.-K. Lee, B. G. Fox, W. A. Froland, J. D. Lipscomb, E. Münck, *J. Am. Chem. Soc.* **1993**, *115*, 6450–6451.
[11] B. J. Wallar, J. D. Lipscomb, *Chem. Rev.* **1996**, *96*, 2625–2657.
[12] C. E. Tinberg, S. J. Lippard, *Acc. Chem. Res.* **2011**, *44*, 280–288.
[13] M. Merkx, D. A. Kopp, M. H. Sazinsky, J. L. Blazyk, J. Müller, S. L. Lippard, *Angew. Chem. Int. Ed.* **2001**, *40*, 2782–2807; *Angew. Chem.* **2001**, *113*, 2860–2888.
[14] A. C. Rosenzweig, C. A. Frederick, S. J. Lippard, P. Nordlund, *Nature* **1993**, *366*, 537–543.

[15] A. C. Rosenzweig, P. Nordlund, P. M. Takahara, C. A. Frederick, S. J. Lippard, *Chem. Biol.* **1995**, *2*, 409–418.
[16] L. Que Jr., W. B. Tolman, *Nature* **2008**, *455*, 333–340.
[17] P. Nordlund, H. Eklund, *Curr. Opin. Struct. Biol.* **1995**, *5*, 758–766.
[18] C. Krebs, J. M. Bollinger, S. J. Booker, *Curr. Opin. Chem. Biol.* **2011**, *15*, 291–303.
[19] D. Das, B. E. Eser, J. Han, A. Sciore, E. N. G. Marsh, *Angew. Chem. Int. Ed.* **2011**, *50*, 7148–7152; *Angew. Chem.* **2011**, *123*, 7286–7290.
[20] T. M. Makris, C. J. Knoot, C. M. Wilmot, J. D. Lipscomb, *Biochemistry* **2013**, *52*, 6662–6671.
[21] X. Zhang, H. Furutachi, S. Fujinami, S. Nagatomo, Y. Maeda, Y. Watanabe, T. Kitagawa, M. Suzuki, *J. Am. Chem. Soc.* **2005**, *127*, 826–827.
[22] Z. Han, N. Sakai, L. H. Böttger, S. Klinke, J. Hauber, A. X. Trautwein, R. Hilgenfeld, *Structure* **2015**, *23*, 882–892.
[23] K. S. Murray, *Coord. Chem. Rev.* **1974**, *12*, 1–35.
[24] D. M. Kurtz, *Chem. Rev.* **1990**, *90*, 585–606.
[25] L. Que Jr., Y. Dong, *Acc. Chem. Res.* **1996**, *29*, 190–196.
[26] L. Que Jr., *J. Chem. Soc. Dalton Trans.* **1997**, 3933–3940.
[27] M. Costas, K. Chen, L. Que, *Coord. Chem. Rev.* **2000**, *200–202*, 517–544.
[28] L. Que Jr., W. B. Tolman, *Angew. Chem. Int. Ed.* **2002**, *41*, 1114–1137; *Angew. Chem.* **2002**, *114*, 1160–1185.
[29] I. Siewert, C. Limberg, *Chem. Eur. J.* **2009**, *15*, 10316–10328.
[30] J. Du Bois, T. J. Mizoguchi, S. J. Lippard, *Coord. Chem. Rev.* **2000**, *200–202*, 443–485.
[31] E. Y. Tshuva, S. J. Lippard, *Chem. Rev.* **2004**, *104*, 987–1012.
[32] V. C.-C. Wang, S. Maji, P. P.-Y. Chen, H. K. Lee, S. S.-F. Yu, S. I. Chan, *Chem. Rev.* **2017**, *117*, 8574–8621.
[33] S. V. Kryatov, E. V. Rybak-Akimova, S. Schindler, *Chem. Rev.* **2005**, *105*, 2175–2226.
[34] M. Costas, M. P. Mehn, M. P. Jensen, L. Que Jr., *Chem. Rev.* **2004**, *104*, 939–986.
[35] K. Ray, F. F. Pfaff, B. Wang, W. Nam, *J. Am. Chem. Soc.* **2014**, *136*, 13942–13958.
[36] W. N. Oloo, L. Que, *Acc. Chem. Res.* **2015**, *48*, 2612–2621.
[37] R. Robson, *Inorg. Nucl. Chem. Lett.* **1970**, *6*, 125–128.
[38] R. Robson, *Aust. J. Chem.* **1970**, *23*, 2217–2224.
[39] K.-O. Schäfer, R. Bittl, W. Zweygart, F. Lendzian, G. Haselhorst, T. Weyhermüller, K. Wieghardt, W. Lubitz, *J. Am. Chem. Soc.* **1998**, *120*, 13104–13120.
[40] A. S. Borovik, M. P. Hendrich, T. R. Holman, E. Münck, V. Papaefthymiou, L. Que Jr., *J. Am. Chem. Soc.* **1990**, *112*, 6031–6038.
[41] K. D. Karlin, Z. Tyeklar, A. Farooq, M. S. Haka, P. Ghosh, R. W. Cruse, Y. Gultneh, J. C. Hayes, P. J. Toscano, J. Zubieta, *Inorg. Chem.* **1992**, *31*, 1436–1451.
[42] M. Kodera, Y. Kawahara, Y. Hitomi, T. Nomura, T. Ogura, Y. Kobayashi, *J. Am. Chem. Soc.* **2012**, *134*, 13236–13239.
[43] M. Kodera, H. Shimakoshi, K. Kano, *Chem. Commun.* **1996**, 1737–1738.
[44] M. Kodera, M. Itoh, K. Kano, T. Funabiki, M. Reglier, *Angew. Chem. Int. Ed.* **2005**, *44*, 7104–7106; *Angew. Chem.* **2005**, *117*, 7266–7268.
[45] J. B. H. Strautmann, S. Dammers, T. Limpke, J. Parthier, T. P. Zimmermann, S. Walleck, G. Heinze-Brückner, A. Stammler, H. Bögge, T. Glaser, *Dalton Trans.* **2016**, *45*, 3340–3361.
[46] J. B. H. Strautmann, S. Walleck, H. Bögge, A. Stammler, T. Glaser, *Chem. Commun.* **2011**, *47*, 695–697.
[47] T. Limpke, C. Butenuth, A. Stammler, H. Bögge, T. Glaser, *Eur. J. Inorg. Chem.* **2017**, *2017*, 3570–3579.
[48] S. Dammers, T. P. Zimmermann, S. Walleck, A. Stammler, H. Bögge, E. Bill, T. Glaser, *Inorg. Chem.* **2017**, *56*, 1779–1782.
[49] Y. Zang, G. Pan, L. Que Jr., B. G. Fox, E. Munck, *J. Am. Chem. Soc.* **1994**, *116*, 3653–3654.
[50] Y. Zang, Y. Dong, L. Que Jr., K. Kauffmann, E. Muenck, *J. Am. Chem. Soc.* **1995**, *117*, 1169–1170.
[51] Y. Dong, H. Fujii, M. P. Hendrich, R. A. Leising, G. Pan, C. R. Randall, E. C. Wilkinson, Y. Zang, L. Que Jr., *J. Am. Chem. Soc.* **1995**, *117*, 2778–2792.
[52] Y. Dong, L. Que Jr., K. Kauffmann, E. Muenck, *J. Am. Chem. Soc.* **1995**, *117*, 11377–11378.
[53] Y. Dong, Y. Zang, L. Shu, E. C. Wilkinson, L. Que Jr., K. Kauffmann, E. Münck, *J. Am. Chem. Soc.* **1997**, *119*, 12683–12684.
[54] H.-F. Hsu, Y. Dong, L. Shu, V. G. Young, L. Que Jr., *J. Am. Chem. Soc.* **1999**, *121*, 5230–5237.
[55] H. Zheng, S. J. Yoo, E. Münck, L. Que, *J. Am. Chem. Soc.* **2000**, *122*, 3789–3790.
[56] G. Xue, D. Wang, R. de Hont, A. T. Fiedler, X. Shan, E. Münck, L. Que Jr., *Proc. Natl. Acad. Sci. USA* **2007**, *104*, 20713–20718.
[57] X. Shan, L. Que, *Proc. Natl. Acad. Sci. USA* **2005**, *102*, 5340–5345.
[58] G. Xue, A. T. Fiedler, M. Martinho, E. Munck, L. Que Jr., *Proc. Natl. Acad. Sci. USA* **2008**, *105*, 20615–20620.
[59] G. Xue, R. de Hont, E. Münck, L. Que Jr., *Nat. Chem.* **2010**, *2*, 400–405.
[60] M. Martinho, G. Xue, A. T. Fiedler, L. Que Jr., E. L. Bominaar, E. Münck, *J. Am. Chem. Soc.* **2009**, *131*, 5823–5830.
[61] A. Hazell, K. B. Jensen, C. J. McKenzie, H. Toftlund, *Inorg. Chem.* **1994**, *33*, 3127–3134.
[62] J. B. H. Strautmann, C.-G. Freiherr von Richthofen, G. Heinze-Brückner, S. DeBeer, E. Bothe, E. Bill, T. Weyhermüller, A. Stammler, H. Bögge, T. Glaser, *Inorg. Chem.* **2011**, *50*, 155–171.
[63] J. B. H. Strautmann, S. D. George, E. Bothe, E. Bill, T. Weyhermüller, A. Stammler, H. Bögge, T. Glaser, *Inorg. Chem.* **2008**, *47*, 6804–6824.
[64] T. Glaser, R. H. Pawelke, M. Heidemeier, *Z. Anorg. Allg. Chem.* **2003**, *629*, 2274–2281.
[65] J. B. H. Strautmann, C.-G. Freiherr von Richthofen, S. DeBeer George, E. Bothe, E. Bill, T. Glaser, *Chem. Commun.* **2009**, 2637–2639.
[66] T. Glaser, *Coord. Chem. Rev.* **2019**, *380*, 353–377.
[67] C. Würtele, F. W. Heinemann, S. Schindler, *J. Coord. Chem.* **2010**, *63*, 2629–2641.
[68] M. Aschenbrenner, A. Stammler, H. Bögge, T. Glaser, *Z. Anorg. Allg. Chem.* **2018**, *644*, 1439–1444.
[69] T. P. Zimmermann, T. Limpke, A. Stammler, H. Bögge, S. Walleck, T. Glaser, *Inorg. Chem.* **2018**, *57*, 5400–5405.
[70] T. P. Zimmermann, T. Limpke, A. Stammler, H. Bögge, S. Walleck, T. Glaser, *Z. Anorg. Allg. Chem.* **2018**, *644*, 683–691.
[71] T. P. Zimmermann, T. Limpke, N. Orth, A. Franke, A. Stammler, H. Bögge, S. Walleck, I. Ivanovic-Burmazovic, T. Glaser, *Inorg. Chem.* **2018**, *57*, 10457–10468.
[72] T. P. Zimmermann, S. Dammers, A. Stammler, H. Bögge, T. Glaser, *Eur. J. Inorg. Chem.* **2018**, *48*, 5229–5237.
[73] K. J. Nelson, A. G. Dipasquale, A. L. Rheingold, M. C. Daniels, J. S. Miller, *Inorg. Chem.* **2008**, *47*, 7768–7774.
[74] J. Reedijk, *Comm. Inorg. Chem.* **1982**, *1*, 379–389.
[75] P. A. Goodson, A. R. Oki, J. Glerup, D. J. Hodgson, *J. Am. Chem. Soc.* **1990**, *112*, 6248–6254.
[76] Y. Hayashi, T. Kayatani, H. Sugimoto, M. Suzuki, K. Inomata, A. Uehara, Y. Mizutani, T. Kitagawa, Y. Maeda, *J. Am. Chem. Soc.* **1995**, *117*, 11220–11229.

[77] H. Nagao, N. Komeda, M. Mukaida, M. Suzuki, K. Tanaka, *Inorg. Chem.* **1996**, *35*, 6809–6815.
[78] L. Benhamou, M. Lachkar, D. Mandon, R. Welter, *Dalton Trans.* **2008**, 6996–7003.
[79] M. Suzuki, *Acc. Chem. Res.* **2007**, *40*, 609–617.
[80] I. Prat, A. Company, T. Corona, T. Parella, X. Ribas, M. Costas, *Inorg. Chem.* **2013**, *52*, 9229–9244.
[81] Y. Zang, J. Kim, Y. Dong, E. C. Wilkinson, E. H. Appelman, L. Que Jr., *J. Am. Chem. Soc.* **1997**, *119*, 4197–4205.
[82] H. Hayashi, K. Uozumi, S. Fujinami, S. Nagatomo, K. Shiren, H. Furutachi, M. Suzuki, A. Uehara, T. Kitagawa, *Chem. Lett.* **2002**, *31*, 416–417.
[83] M. Mizuno, H. Hayashi, S. Fujinami, H. Furutachi, S. Nagatomo, S. Otake, K. Uozumi, M. Suzuki, T. Kitagawa, *Inorg. Chem.* **2003**, *42*, 8534–8544.
[84] R. C. Holz, T. E. Elgren, L. L. Pearce, J. H. Zhang, C. J. O′Connor, L. Que Jr., *Inorg. Chem.* **1993**, *32*, 5844–5850.
[85] L. H. Do, G. Xue, L. Que Jr., S. J. Lippard, *Inorg. Chem.* **2012**, *51*, 2393–2402.
[86] H. Zheng, Y. Zang, Y. Dong, V. G. Young, L. Que Jr., *J. Am. Chem. Soc.* **1999**, *121*, 2226–2235.
[87] S. V. Kryatov, E. V. Rybak-Akimova, *J. Chem. Soc. Dalton Trans.* **1999**, 3335–3336.
[88] S. A. Stoian, G. Xue, E. L. Bominaar, L. Que, E. Münck, *J. Am. Chem. Soc.* **2014**, *136*, 1545–1558.
[89] A. J. Skulan, T. C. Brunold, J. Baldwin, L. Saleh, J. M. Bollinger, E. I. Solomon, *J. Am. Chem. Soc.* **2004**, *126*, 8842–8855.
[90] M. N. Mortensen, B. Jensen, A. Hazell, A. D. Bond, C. J. McKenzie, *Dalton Trans.* **2004**, 3396–3402.
[91] H. Kurosaki, H. Yoshida, M. Ito, H. Koike, E. Higuchi, M. Goto, *Bioorg. Med. Chem. Lett.* **2001**, *11*, 785–788.
[92] R. E. Norman, R. C. Holz, S. Menage, C. J. O′Connor, J. H. Zhang, L. Que Jr., *Inorg. Chem.* **1990**, *29*, 4629–4637.
[93] S. Taktak, S. V. Kryatov, E. V. Rybak-Akimova, *Inorg. Chem.* **2004**, *43*, 7196–7209.
[94] T. Beissel, F. Birkelbach, E. Bill, T. Glaser, F. Kesting, C. Krebs, T. Weyhermüller, K. Wieghardt, C. Butzlaff, A. X. Trautwein, *J. Am. Chem. Soc.* **1996**, *118*, 12376–12390.
[95] M. Born, *Z. Phys.* **1920**, *1*, 45–48.
[96] A. Bencini, D. Gatteschi, *Electron Paramagnetic Resonance of Exchanged Coupled Systems*, Springer, Berlin, **1990**.
[97] S. Walleck, T. P. Zimmermann, A. Stammler, H. Bögge, T. Glaser, *unpublished results*.
[98] T. P. Zimmermann, N. Orth, S. Finke, T. Limpke, A. Stammler, H. Bögge, S. Walleck, I. Ivanovic-Burmazovic, T. Glaser, *manuscript in preparation*.

Manuscript received: August 12, 2019
Revised manuscript received: November 25, 2019
Version of record online: January 16, 2020

